Identification of Asp 549 as the Catalytic Nucleophile of Glycogen-Debranching Enzyme via Trapping of the Glycosyl−Enzyme Intermediate†

Curtis Braun,‡ Thisbe Lindhorst,‡ Neil B. Madsen,§ and Stephen G. Withers*,‡,||

Department of Chemistry, University of British Columbia, 2036 Main Mall, Vancouver, British Columbia, Canada V6T 1Z1, Department of Biochemistry, University of British Columbia, Vancouver, British Columbia, Canada V6T 1Z3, and Department of Biochemistry, University of Alberta, Edmonton, Alberta, Canada T6G 2H7

Received November 7, 1995; Revised Manuscript Received January 30, 1996⊗

ABSTRACT: Glycogen-debranching enzyme catalyzes the removal of branching from glycogen via a two-step process involving first the transfer of a maltotriosyl unit from the branch to the main chain and second the hydrolysis of the residual α-(1,6)-linked glucose moiety. Since the transfer occurs with retention of anomeric configuration, a mechanism involving a maltotriosyl−enzyme species is presumed. 4-Deoxy-α-maltotriosyl fluoride functions as an incompetent substrate for this transferase activity since a glycosyl−enzyme species is formed, as witnessed by a "burst" of fluoride release, but turned over only very slowly unless a suitable acceptor such as maltotriose is added, at which point 4-deoxymaltohexaose is released. Peptic proteolysis of this trapped enzyme generated a mixture of peptides which was separated by reverse phase high-performance liquid chromatography, and the glycosylated peptide was located by use of tandem mass spectrometry in the neutral loss mode. Subsequent tandem mass spectrometric experiments on this peptide identified it as one surrounding Asp 549. This amino acid is completely conserved in all α-glucanotransferases and α-glucosidases belonging to this sequence-related family and is hereby identified as the catalytic nucleophile.

Glycogen-debranching enzyme (Glix,[1] amylo-1,6-glucosidase [EC 3.2.1.33]/4-α-glucanotransferase [EC 2.2.1.25]) plays an important role in carbohydrate metabolism, working in conjunction with glycogen phosphorylase in the total degradation of glycogen. Glycogen phosphorylase removes glucose units from glycogen via phosphorolysis of the α-(1,4) chains to within four residues of a branch point. Glix then removes the α-(1,6) branch points from this limit dextrin by a two-step process as shown in Figure 1. In the first step, a glycosyl transferase activity transfers a maltotriose unit from the four-sugar branch to the "main" chain, resulting in an elongated section of α-(1,4) polymer, with a single glucose attached to it via an α-(1,6) linkage. The enzyme then utilizes a glucosidase activity to hydrolyze the glucose stub, thus allowing glycogen phosphorylase to continue degradation of the linearized α-(1,4) polymer. Both the transferase and the glucosidase activities are found on a single polypeptide chain (Brown & Brown, 1966; Nelson et al., 1979) that has recently been determined to have a molecular weight of 177 542 Da (Liu et al., 1993) (rabbit muscle).

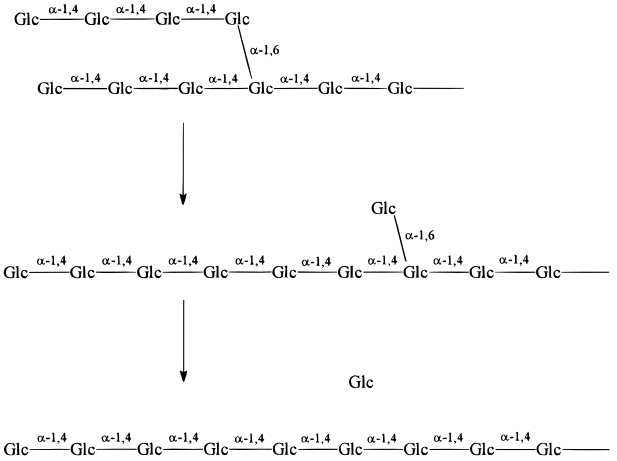

FIGURE 1: Removal of the branch point from limit dextrin by glycogen-debranching enzyme.

Thus, Glix catalyzes two separate reactions. The first of these is a glycosyl transfer in which an α-(1,4) bond is cleaved and a new α-(1,4) bond is formed. Since this occurs with net retention of anomeric configuration, it most likely involves a double displacement mechanism. The second reaction is that of an α-glucosidase in which an α-(1,6) glucoside linkage is hydrolyzed. Previous studies (Liu et al., 1991) demonstrated that this reaction occurs with net inversion of anomeric configuration, most likely via a single displacement mechanism.

Withers et al. (1988) have shown that 2-deoxy-2-fluoroglycosides rapidly inactivate "retaining" *β*-glycosidases by forming highly stabilized glycosyl−enzyme intermediates. They therefore act as useful probes for studying the reaction mechanism of these enzymes. Unfortunately, α-glycosidases

† Financial support from the Natural Sciences and Engineering Research Council of Canada and a fellowship (to T.L.) from the Deutsche Forschungsgemeinschaft are gratefully acknowledged.

* To whom correspondence should be addressed. Telephone: 604-822-3402. Fax: 604-822-2847. E-mail: withers@unixg.ubc.ca.

‡ Department of Chemistry, University of British Columbia.

§ University of Alberta.

|| Department of Biochemistry, University of British Columbia.

⊗ Abstract published in *Advance ACS Abstracts,* April 1, 1996.

[1] Abbreviations: MS/MS, tandem electrospray mass spectrometry; Glix, glycogen-debranching enzyme; 4DαG3F, 4-deoxy-α-maltotriosyl fluoride; 4DG5, 4-deoxymaltopentaose; 4DG6, 4-deoxymaltohexaose; MALDI−TOF, matrix-assisted laser desorption ionization−time of flight; TFA, trifluoroacetic acid; CGT, collision gas thickness; SDS−PAGE, sodium dodecyl sulfate−polyacrylamide gel electrophoresis; ESMS, electrospray ionization mass spectrometry; LC/MS, liquid chromatography/mass spectrometry; *m/z*, mass/charge ratio; TIC, total ion chromatogram.

S0006-2960(95)02648-1 CCC: $12.00

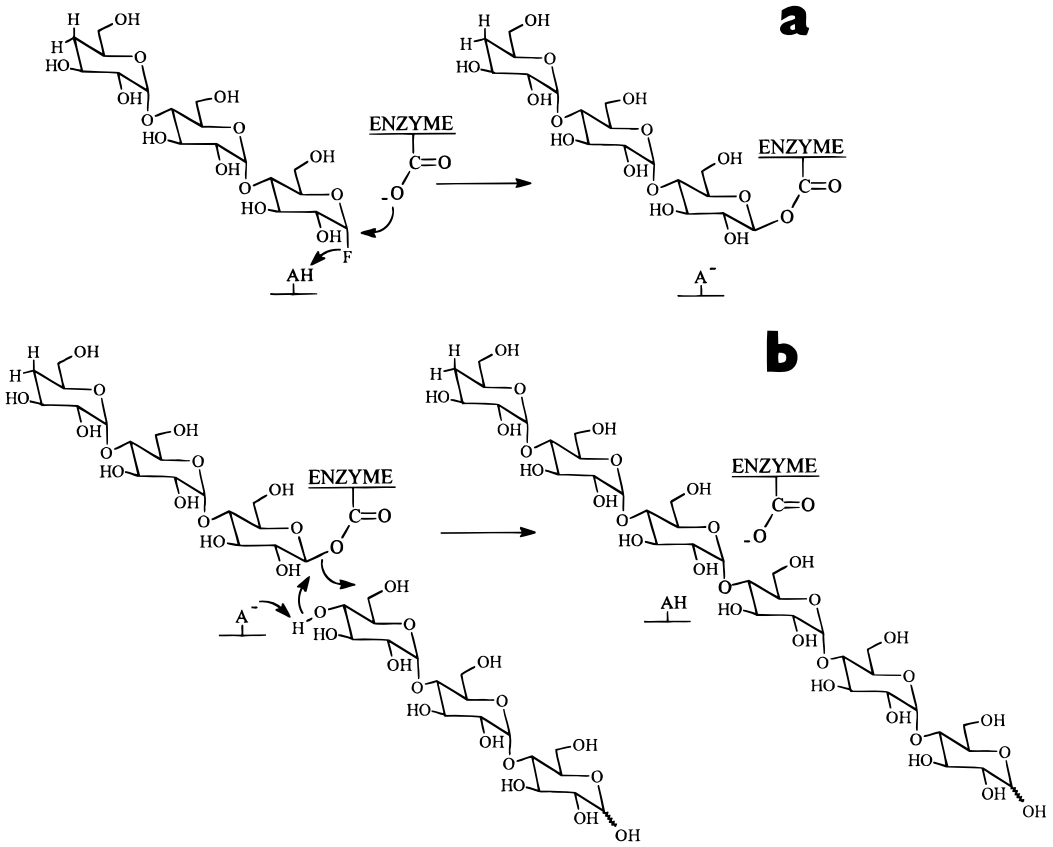

FIGURE 2: Mechanism for the accumulation of an intermediate on Glix in the presence of 4DαG3F and subsequent turnover via transglycosylation upon addition of maltotriose.

do not appear to be susceptible to such an inactivation strategy, as suggested early on (Withers et al., 1988) and substantiated subsequently (Braun, 1995). This inactivity is likely due to the second step in the α-glycosidase mechanism (cleavage of a β-linked intermediate) being faster than the first step, which involves cleavage of the α-glycoside. Trapping the intermediate is therefore more difficult. This was also true for Glix since 2-deoxy-2-fluoro-α-maltotriosyl fluoride was tested as a mechanism-based inhibitor of the transferase activity but was found to act only as a slow substrate, no accumulation of enzyme intermediate being observed (McCarter et al., 1993).

The aim of this study was to design a different approach to accumulation of the glycosyl−enzyme intermediate in glycosyl transferases such as glycogen-debranching enzyme and to use this approach to identify the nucleophile at the active site. This approach is based upon our earlier finding (Braun & Withers, 1995) that maltotriosyl fluoride functions as a good substrate (k_{cat} = 31 min^{-1}) for the transferase activity of Glix, the reaction occurring via transglycosylation and resulting in the formation of elongated maltooligosaccharyl fluorides. Therefore, if a maltotriosyl fluoride substrate which is deoxygenated at the 4-position is added to the enzyme, the first step (glycosylation) will occur at the transferase site, but the second step (deglycosylation) will not. An intermediate should therefore accumulate as shown in Figure 2a. Subsequent addition of a maltooligosaccharide with a 4-hydroxyl group should result in turnover of this intermediate as shown in Figure 2b. 4-Deoxy-α-maltotriosyl fluoride was thus synthesized (Lindhorst et al., 1995) and tested for its ability to trap an intermediate at the transferase site of glycogen-debranching enzyme.

MATERIALS AND METHODS

Glycogen-debranching enzyme was purified from rabbit muscle as described previously (Takrama & Madsen, 1988). 4DαG3F was synthesized as described (Lindhorst et al., 1995). All other chemicals were obtained from Sigma Chemical Co., unless otherwise indicated, and were used without further purification.

The reaction of Glix with 4DαG3F was monitored by following the release of fluoride ion using an Orion ion selective fluoride ion electrode. To 4DαG3F (150 μL, 3.1 mM) in 100 mM sodium phosphate and 1 mM ethylenediaminetetraacetic acid (EDTA) buffer at pH 6.0 and 30 °C was added glycogen-debranching enzyme (100 μL, 28.3 mg/mL). Maltotriose (6 mg) was added after the burst phase had been achieved and reaction had reached a steady state. Purification of products was performed using a Dextropak high-performance liquid chromatography (HPLC) column from Waters run in deionized water at room temperature. Identification of oligosaccharide products was achieved using a Kratos MALDI−TOF mass spectrometer. The spectrometer was calibrated using the external standard maltotetraose.

Labeling of glycogen-debranching enzyme (8 μL, 28 mg/mL) was achieved by incubation of the enzyme with 4DαG3F (2 μL, 100 mM) for 10 min under the same conditions as described for the burst experiment above. The enzyme was digested by addition of 32 μL of 50 mM sodium phosphate buffer (pH 2) and 10 μL of pepsin (0.5 mg/mL) in pH 2 buffer, and the mixture was incubated at room temperature for 1 h. SDS−PAGE analysis confirmed that glycogen-debranching enzyme was completely digested under these conditions.

Analysis of the proteolytic digests was carried out using a Sciex API-III electrospray ionization mass spectrometer interfaced with a Michrom UMA HPLC system (Michrom BioResources Inc., Pleasanton, CA). A sample of the digest (10 μL, 4.3 mg/mL) was loaded onto a C18 column (Reliasil, 1 × 150 mm) and then eluted at a flow rate of 50 μL/min with a gradient of 0 to 60% solvent B/100 to 40% solvent A over 20 min followed by 100% B for 2 min (solvent A, 0.05% TFA and 2% acetonitrile in water; solvent B, 0.045% TFA and 80% acetonitrile in water). Analysis was first performed in simple LC/MS mode, and then in neutral loss mode, using the following conditions.

The single quadrupole mode (normal LC/MS) MS conditions were as follows. The quadrupole mass analyzer was scanned over a *m*/*z* range of 300−2400 Da with a step size of 0.5 Da and a dwell time of 1 ms/step. ISV was set at 5 kV, and the orifice energy (OR) was 80 V. The neutral loss MS/MS spectra were obtained in the triple quadrupole neutral loss scan mode searching for the loss of *m*/*z* 235.5, corresponding to the loss of inhibitor label from a peptide in the doubly charged state. Thus, scan range = 300−1200 *m*/*z*, step size = 0.5 Da, dwell time = 1 ms/step, ISV = 5 kV, OR = 80 V, RE1 = 115, DM1 = 0.16, R1 = 0 V, R2 = −50 V, RE3 = 115, DM3 = 0.16, and CGT = 3.2−3.6 × 10^{14} molecules/cm^2. To maximize the sensitivity of neutral loss detection, normally the resolution (RE and DM) is compromised without generation of artifact neutral loss peaks.

The MS/MS daughter ion spectrum of the selected peak was obtained in the triple quadrupole daughter ion scan mode by selective introduction of the *m*/*z* 1081 or 1321 doubly charged peptide from Q1 into the collision cell (Q2) and observation of the daughter ions in Q3. Thus, Q1 was locked on *m*/*z* 1081 or 1321, Q3 scan range = 300−2400 *m*/*z*, step size = 1.0 Da, dwell time = 1 ms/step, ISV = 5 kV, OR = 80 V, RE1 = 112, DM1 = 0.18, R1 = 0 V, R2 = −50V, RE3 = 112, DM3 = 0.18, and CGT = 4.5 × 10^{14} molecules/cm^2. All MS data were analyzed using Sciex BioToolbox software.

Conversion of the ester-linked labeled peptide to an amide at that position was carried out by addition of 2 μL of concentrated ammonium hydroxide to the peptic digest (10 μL, 5 mg/mL) and incubation at 50 °C for 15 min. After acidification with TFA, the mixture was analyzed by ESMS.

RESULTS AND DISCUSSION

Burst Experiment. Reaction of 4DαG3F with Glix was monitored using a fluoride ion selective electrode. As can be seen in Figure 3, addition of 41 μM Glix to an excess (1.8 mM) of 4DαG3F resulted in the relatively rapid initial release of fluoride followed by a slower steady state reaction. The quantity of fluoride released in this initial phase was estimated by extrapolation of the linear portion of the plot back to $t = 0$, yielding a value of 43 μM fluoride released. This corresponds well with the amount of enzyme present (41 μM), suggesting that this is indeed a true burst of fluoride arising from reaction of 1 equiv of 4DαG3F with the enzyme. The second, steady state phase presumably arises from slow hydrolysis of the accumulated intermediate. The experiment was repeated with half the amount of enzyme, and similar results were seen except that the burst was half the size (data not shown).

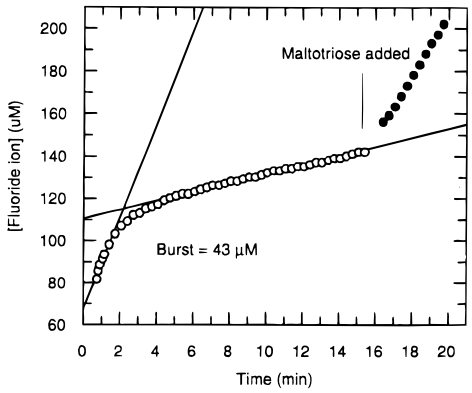

FIGURE 3: Reaction of 4DαG3F with Glix (○). Addition of 100 μL of debranching enzyme (41 μM) to 150 μL of 4DαG3F (1.8 mM) in 100 mM phosphate and 1 mM EDTA buffer (pH 6.90). (●) After 16 min, maltotriose (6.5 mg) was added.

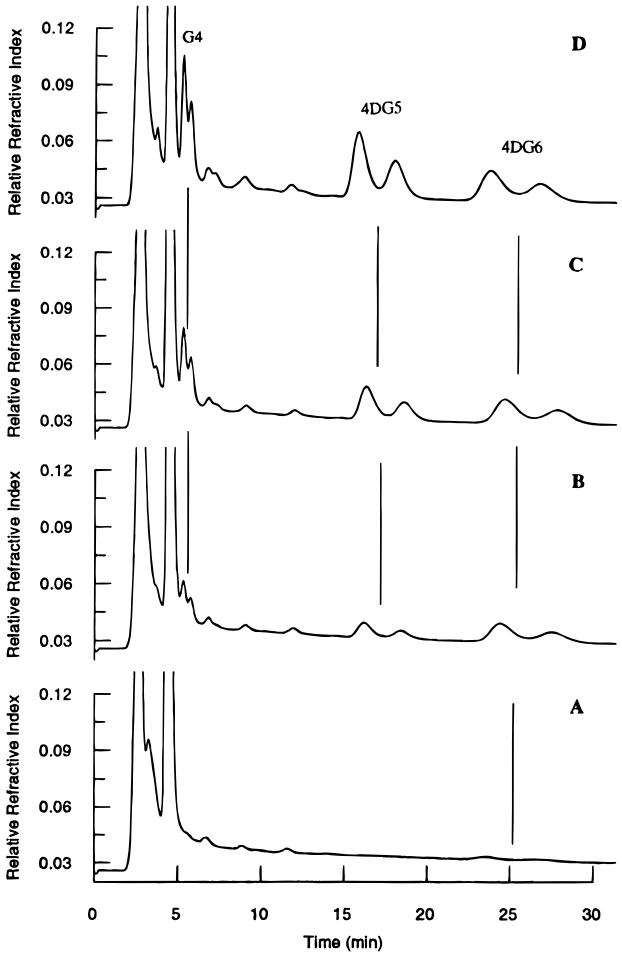

FIGURE 4: HPLC profiles of the products formed from the reaction of 4DαG3F with Glix in the presence of maltotriose. Reaction times after enzyme addition were as follows: (A) 5.5 min, (B) 96 min, (C) 186 min, and (D) 366 min.

Accumulation of an intermediate occurs because no sugar molecule with a free 4-hydroxyl group is present to act as an acceptor. Therefore, addition of an appropriate acceptor should result in an increase in the steady state rate via a transglycosylation process, thereby providing further evidence for the existence of a trapped glycosyl−enzyme intermediate. Such an experiment is shown in Figure 3, where addition of maltotriose to this trapped enzyme resulted in a dramatic increase in the rate of fluoride release, presumably via a transglycosylation reaction. Confirmation

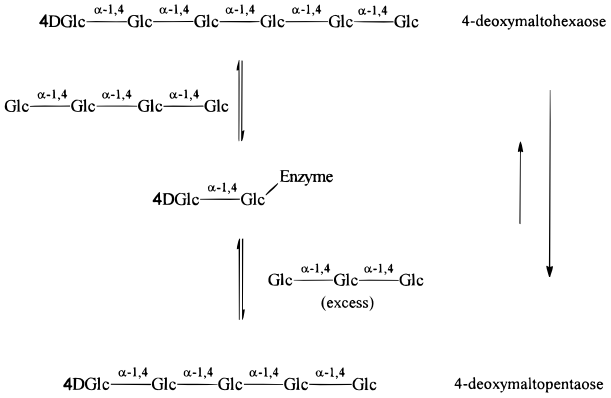

FIGURE 5: Disproportionation of 4DG6 by Glix in the presence of excess maltotriose.

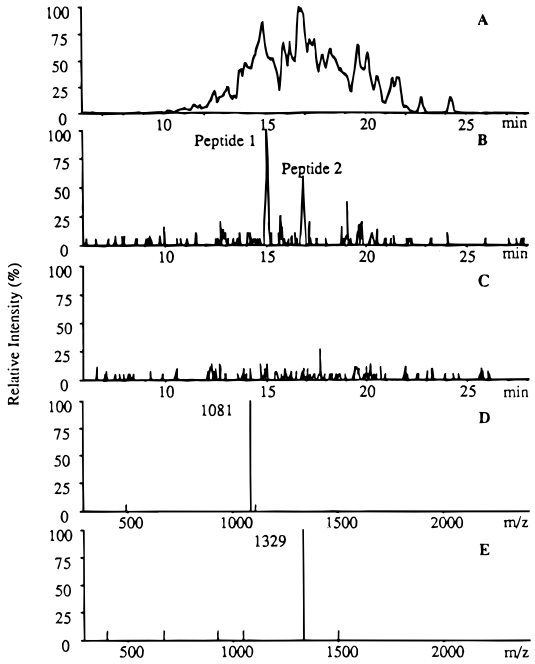

FIGURE 6: ESMS/MS experiments on Glix proteolytic digests: (A) labeled with 4DαG3F, TIC in normal MS mode; (B) labeled with 4DαG3F, TIC in neutral loss mode; (C) unlabeled, in neutral loss mode; (D) mass spectrum of peptide 1 in panel B; and (E) mass spectrum of peptide 2 in panel B.

of these processes was obtained by product analysis, as follows.

Identification of the Enzymatic Reaction Products. The products of the reaction of 4DαG3F and maltotriose with the debranching enzyme were analyzed by HPLC as shown in Figure 4, in which frames A−D show the reaction time course. Two major products were observed, each as a mixture of anomers, at 17 and 25 min on the HPLC trace. Analysis of these products by MALDI−TOF mass spectrometry indicated that the product formed first, the doublet at 25 min, has a mass of $m/z = 997.2 \pm 1.0$. This agrees closely with the theoretical m/z for 4DG6, the expected product (4DG6 + Na^+ = 997.9) (Figure 2).

This is closely followed by another product, which later becomes the major species. This reaction product, at 17 min in the HPLC traces, was determined to be 4DG5 (4DG5 + Na^+ = 835.7) by MALDI−TOF mass spectrometry. This product presumably results from a disproportionation reaction as shown in Figure 5, a process which Glix is known to catalyze (Brown & Brown, 1966; Tabata & Dohi, 1992).

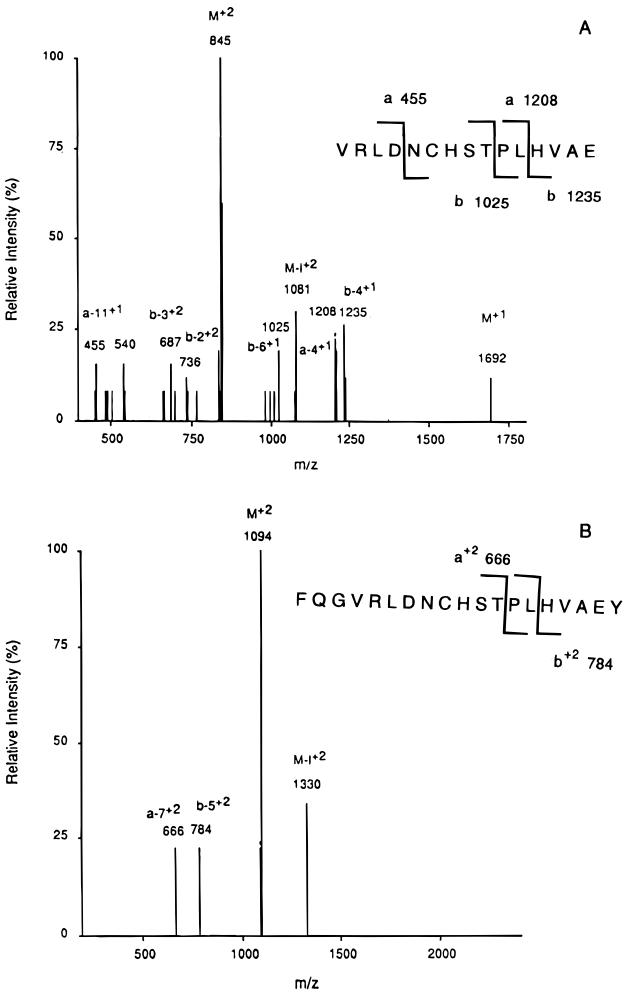

FIGURE 7: Tandem MS/MS daughter ion spectrum of the 4DαG3F-labeled active site peptides: (A) peptide 1 (*m/z* 1081, in the doubly charged state) and (B) peptide 2 (*m/z* 1329, in the doubly charged state).

Therefore, as 4DG6 accumulates, the debranching enzyme uses it as a substrate, cleaving off maltotetraose and forming a 4-deoxymaltosyl−enzyme intermediate. Maltotriose (present in large excess) then acts as the acceptor, resulting in the formation of 4DG5. The appearance of 4DG5 should therefore be accompanied by the appearance of maltotetraose. This is indeed the case, as is seen in Figure 4 where maltotetraose appears as a doublet at 6 min in the HPLC profiles.

The product of the reaction observed in the presence of 4DαG3F, but in the absence of maltotriose, under steady state conditions was identified to be 4-deoxymaltotriose by similar HPLC analysis using an authentic standard (Lindhorst et al., 1995) (data not shown). The steady state turnover observed is therefore a consequence of the transferase site slowly allowing water to act as the acceptor, resulting in hydrolysis of the intermediate.

Identification of the Peptide Containing the Catalytic Nucleophile. Identification of the site of attachment of the 4-deoxymaltotriosyl moiety was achieved by use of a tandem mass spectrometric method recently developed for such a purpose (Henderson et al., 1992; Hunt et al., 1992; Miao et al., 1994a,b; Tull et al., 1995). This method relies upon the expectation that the sugar will be linked to the protein via an ester linkage with the side chain carboxyl group of an aspartic or glutamic acid, as has been found for all glycosi-

	Consensus Sequence 1	Consensus Sequence 2	Consensus Sequence 3	Consensus Sequence 4
α-Amylase				
Aspergillus oryzae	111 GMYLMVDVVANH	201 DGLRIDTVKH	226 YCIGEVLD	289 LGTFVENHD
Barley 1	82 GVQAIADIVINH	175 DAWRLDFARG	201 LAVAEVWD	283 AATFVDNHD
Drosophila melanogaster	88 GVRTYVDVVFNH	181 AGFRVDAAKH	219 YIVQEVID	279 SLVFVDNHD
Porcine pancreas	90 GVRIYVDAVINH	192 AGFRLDASKH	229 FIFQEVID	292 ALVFVDNHD
Human pancreas	90 GVRIYVDAVINH	192 AGFRLDASKH	229 FIFQEVID	292 ALVFVDNHD
α-Glucosidase				
Saccharomyces cerevisiae	100 GMKFITDLVINH	170 DGFRIDTAGL	272 MRVGEVAH	341 ATTYIENHD
α-Glucosyltransferase (GTase-I)				
Streptococcus sobrinus		DSIRVDAVD		
Cyclodextrinase				
Bacillus sphaericus	232 GMRVLLDAVFNH	321 DGWRLDVANE	351 YILGEIMH	414 SFNLLGSHD
Pullulanase				
Klebsiella pneumonia	596 GMNVIMDVVYNH	672 DGFRFDLMGY	702 YFFGEGWD	826 VVNYVSKHD
Isoamylase				
Pseudomonas amyloderamosa	298 GIKVYMDVVYNH	369 DGFRFDLASV	412 RILREFTV	499 SINFIDVHD
Oligo-1,6-glucosidase				
Bacillus cereus	92 NHKLMMDLVVNH	194 DGFRMDVINF	251 MTVGEMPG	321 NSLYWNNHD
Cyclodextrin glucanotransferase				
Bacillus macerans	129 NIKVVMDFAPNH	224 DGIRFDAVKH	254 FTFGEWFL	321 MVTFIDNHD
Branching enzyme				
Escherichia coli	328 GLNVILDWVPGH	399 DALRVDAVAS	453 VTMAEEST	517 NFVLPLNHD
Amylomaltase				
Streptococcus pneumonia	218 VAEDSSDMWAND	290 DIVRIDHFRG	328 AAVKEELG	388 SVMYTGTHD
Glycogen debranching enzyme				
Human muscle	192 NVICITDVVYNH	504 QGVRLDNCHS	534 YVVAELFT	602 ALFMDITHD
Rabbit muscle	232 NVLCITDVVYNH	544 QGVRLDNCHS	574 YVVAELFT	642 ALFMDITHD
	Sequence of labeled peptide:	VRLDNCHSTPLHVAE		

FIGURE 8: Identified labeled peptide and the conserved sequence in the α-amylase superfamily.

dases reliably labeled to date (McCarter & Withers, 1994). Such an ester linkage is known to fragment in the collision cell of a mass spectrometer with loss of a neutral sugar moiety, leaving the peptide to which it was attached with its same charge but a lower mass. A peptide bearing an ester-linked sugar can therefore be identified in a proteolytic digest by means of a neutral loss scan, as follows. Glix was incubated with 4DαG3F for 10 min until all the enzyme was in the 4-deoxymaltotriosyl−enzyme form and then digested using the protease pepsin. The mixture of peptides produced was partially separated by reverse-phase HPLC, using the ESMS as the detector. When the spectrometer was scanned in the normal LC/MS mode, the TIC of the digest displays a very large number of peptides, as expected from a protein of this size (177 kDa) (Figure 6A). In order to determine which peptide(s) had the trisaccharide attached, a second run was performed using the tandem mass spectrometer set up in the neutral loss mode, searching for a peptide which loses a neutral species of mass 471 Da, this being the mass of the 4-deoxymaltotriosyl moiety. The two quadrupoles were therefore first scanned in a linked fashion such that only ions that differed by a mass of 471 (singly charged species) could pass through both quadrupoles and be detected. However, no significant peak was observed. By contrast, good results were obtained when the neutral loss scan was repeated, but searching for a loss of $m/z = 235.5$, corresponding to the loss of the inhibitor label from a peptide ion in the doubly charged state. Results are shown in Figure 6B, along with the results of a similar experiment carried out on a peptic digest of unlabeled enzyme (Figure 6C). Comparison of the two neutral loss profiles shows two distinct peaks which were present in the labeled experiment and not present in the control, labeled as peptide 1 and peptide 2 in Figure 6B. These two doubly charged, labeled peptides were shown to have *m/z* values of 1081 (±1) and 1329 (±1), respectively. These correspond to unlabeled peptides of molecular weight 1692 (±2) [(2 × 1081) − 471 + 1H] and 2188 (±2) [(2 × 1329) − 471 + 1H]. A search through the amino acid sequence of the debranching enzyme (Liu et al., 1993) using the Sciex BioToolbox software revealed that a total of 48 and 45 peptides, respectively, could be derived from Glix that could satisfy the molecular weights of peptide 1 and peptide 2. Assuming that the two peptides observed arise from alternate modes of proteolysis of the same labeled protein and that the peptide of interest will contain a glutamic or aspartic acid residue, then comparison of these two lists reveals possible sites of labeling which are common to both. Further identification was obtained as follows.

Sequence information was obtained, without further purification, by additional fragmentation of peptide 1 in the daughter ion scan mode. The parent ion of *m/z* 1081 (doubly charged state) was selected in the first quadrupole and subjected to collision-induced fragmentation in a collision cell in the second quadrupole. The masses of the daughter ions produced were detected in the third quadrupole. The mass spectrum obtained is shown in Figure 7A. The daughter ion at *m/z* 845 arises from the loss of the 4-deoxymaltotriosyl label from the doubly charged parent. All the daughter ions that are at *m/z* higher than 845 must therefore correspond to singly charged peptides arising from further fragmentation. Thus, the peptide at $m/z = 1692$ corresponds to the singly charged peptide which has lost its sugar label plus one proton. Sciex BioToolbox software was used to predict fragmentation patterns for all 48 possible peptides, and only one was found which could have given rise to the fragmentation pattern observed. The sequence of this peptide was ^{546}VRLDNCHSTPLHVAE^{560} corresponding to residues Val 546 to Glu 560. The fragmentation pattern of the labeled peptide arises as follows. The peaks at *m/z* 1235/1208 are attributed to the loss of the C-terminal tetrapeptide HVAE. The peaks at *m/z* 1025 and 455 resulted from the C-terminal loss of PLHVAE and NCHSTPLHVAE, respectively. The other peaks at *m/z* 736 and 687 resulted from equivalent C-terminal losses of AE and VAE from the peptide in the doubly charged state.

Peptide 2 (*m*/*z* 1329 in the doubly charged state) was also fragmented in the daughter ion scan mode, and the fragments produced are shown in Figure 7B. The daughter ion at *m*/*z* 1094 arises from the loss of the label from the doubly charged peptide. Even though only two other daughter ions were observed, computer-generated fragmentation patterns of the 45 possible peptides were able to eliminate 40 of these candidates, leaving only five peptides which could have given rise to the two daughter ions observed. Since peptide 1 and peptide 2 both contain the catalytic nucleophile, their sequences must overlap. Of the five remaining peptides, only one overlapped with the sequence of peptide 1. The sequence of this peptide was ^{543}FQGVRLDNCHSTPLHVAEY^{561}.

Identification of the Catalytic Nucleophile. The catalytic nucleophile must be one of the amino acids common to the two peptides. Within these sequences, the only two amino acids which are likely candidates for the nucleophile, on the basis of precedent (Sinnott, 1990; Withers & Aebersold, 1995) and on the basis of the facile fragmentation observed in the mass spectrometer, are Asp 549 and Glu 560.

Covalent attachment of the label to the peptide through an ester linkage was confirmed by aminolysis of the labeled digest. After ammonium hydroxide treatment, the labeled peptide with a peak at *m*/*z* 1081.5 (MH_2^{2+}) was replaced by a new peptide with a peak at *m*/*z* 1691.5 (MH^+). This result is consistent with aminolysis of an ester linkage, thereby converting the nucleophilic amino acid to Asn or Gln and releasing 4-deoxymaltotriose.

Further identification of the catalytic nucleophile came from comparison of the amino acid sequences within the α-amylase family. Recently, it has been concluded, on the basis of sequence alignments, that glycogen-debranching enzyme is a member of the α-amylase superfamily (Liu et al., 1993; Jespersen et al., 1993). Sequence alignments, as shown in Figure 8, reveal that there are four consensus sequences present in the family, with three of the sequences containing the three completely conserved active site carboxylic acids (Svensson, 1994). The labeled peptide was found to be partially contained within one of the consensus sequences as shown in Figure 8. Asp 549 is one of the three completely conserved active site carboxylates, whereas Glu 560 is outside the consensus sequence and is not conserved in any other members of the α-amylase superfamily. Asp 549 also corresponds to the residue suggested to function as the nucleophile on the basis of the crystal structure of the α-amylase from *Aspergillus oryzae* (TAKA) (Matsuura et al., 1984) and to a residue contained in the labeled peptide isolated from the denaturation-trapped α-glucanotransferase from *Streptococcus sobrinus* (Mooser et al., 1991). These data therefore assign Asp 549 as the catalytic nucleophile in the transferase site of rabbit muscle glycogen-debranching enzyme, thereby conclusively assigning the role of this residue in the α-amylase superfamily.

ACKNOWLEDGMENT

We thank Ruedi Aebersold for his generous provision of access to the mass spectrometer and Shichang Miao for his assistance at the early stages. We also thank Shirley Shechosky for preparation of the enzyme.

REFERENCES

Braun, C. (1995) Ph.D. Thesis, University of British Columbia, Cancouver, BC, Canada.
Braun, C., & Withers, S. G. (1995) *Carbohydr. Res. 271*, 113.
Brown, D. H., & Brown, B. I. (1966) *Methods Enzymol. 8*, 515.
Henderson, R. A., Michel, H., Sakaguchi, K., Shabanowitz, J., Appella, E., Hunt, D. F., & Engelhard, V. H. (1992) *Science 255*, 1264.
Hunt, D. F., Henderson, R. A., Shabanowitz, J., Sakaguchi, K., Michel, H., Sevilir, N., Cox, A. L., Appella, E., & Engelhard, V. H. (1992) *Science 255*, 1261.
Jespersen, H. M., MacGregor, E. A., Henrissat, B., Sierks, M. R., & Svensson, B. (1993) *J. Protein Chem. 12*, 791.
Lindhorst, T. K., Braun, C., & Withers, S. G. (1995) *Carbohydr. Res. 268*, 93.
Liu, L., de Castro, L., Takrama, J., Bilous, P. T., Vinayagamoorthy, T., Madsen, N. B., & Bleackley, C. R. (1993) *Arch. Biochem. Biophys. 306*, 232.
Liu, W., Madsen, N. B., Braun, C., & Withers, S. G. (1991) *Biochemistry 30*, 1419.
Matsuura, Y., Kusunoki, M., Harada, W., & Kakudo, M. (1984) *J. Biochem. 95*, 697.
McCarter, J. D., & Withers, S. G. (1994) *Curr. Opin. Struct. Biol. 4*, 361.
McCarter, J. D., Adam, M. J., Braun, C., Namchuk, M., Tull, D., & Withers, S. G. (1993) *Carbohydr. Res., 249*, 77.
Miao, S., McCarter, J. D., Grace, M., Grabowski, G., Aebersold, R., & Withers, S. G. (1994a) *J. Biol. Chem. 269*, 10975.
Miao, S., Ziser, L., Aebersold, R., & Withers, S. G. (1994b) *Biochemistry 33*, 7027.
Mooser, G., Hefta, S. A., Paxton, R. J., Shively, J. E., & Lee, T. D. (1991) *J. Biol. Chem. 266*, 8916.
Nelson, T. E., White, R. C., & Gillard, B. K. (1979) *ACS Symp. Ser. 88*, 131.
Sinnott, M. L. (1990) *Chem. Rev. 90*, 1171.
Svensson, B. (1994) *Plant Mol. Biol. 25*, 141.
Tabata, S., & Dohi, Y. (1992) *Carbohydr. Res. 230*, 179.
Takrama, J., & Madsen, N. B. (1988) *Biochemistry 27*, 3308.
Tull, D., Miao, S., Withers, S. G., & Aebersold, R. (1995) *Anal. Biochem. 224*, 509.
Withers, S. G., & Aebersold, R. (1995) *Protein Sci. 4*, 361.
Withers, S. G., Rupitz, K., & Street, I. P. (1988) *J. Biol. Chem. 263*, 7929.

BI9526488